Site-bond percolation of polyatomic species

M. Dolz*
Centro Atómico Bariloche, CONICET, Avenida Bustillo 9500, 8400 S. C. de Bariloche, Argentina

F. Nieto† and A. J. Ramirez-Pastor‡
Departamento de Física, Universidad Nacional de San Luis, CONICET, Chacabuco 917, 5700 San Luis, Argentina
(Received 31 May 2005; published 30 December 2005)

A generalization of the classical monomer site-bond percolation problem is studied in which linear k-uples of nearest neighbor sites (site k-mers) and linear k-uples of nearest neighbor bonds (bond k-mers) are independently occupied at random on a square lattice. We called this model the site-bond percolation of polyatomic species or k-mer site-bond percolation. Motivated by considerations of cluster connectivity, we have used two distinct schemes (denoted as $S \cap B$ and $S \cup B$) for k-mer site-bond percolation. In $S \cap B(S \cup B)$, two points are said to be connected if a sequence of occupied sites and (or) bonds joins them. By using Monte Carlo simulations and finite-size scaling theory, data from $S \cap B$ and $S \cup B$ are analyzed in order to determine the critical curves separating the percolating and nonpercolating regions.

DOI: 10.1103/PhysRevE.72.066129 PACS number(s): 64.60.Ak, 68.35.Rh, 05.10.Ln

I. INTRODUCTION

The site-bond percolation problem and its applications have been studied for a very long time [1–7]. In a recent contribution, we reported a generalization of the classical site-bond percolation model in which pairs of nearest neighbor sites (site dimers) and linear pairs of nearest neighbor bonds (bond dimers) are independently occupied at random on a square lattice. We called that model the dimer site-bond percolation model [8]. The present paper goes a step further, analyzing the more general model of k-mer site-bond percolation for $k>2$. As was mentioned, a great number of articles have shown the importance of Random Sequential Adsorption (RSA) and the equilibrium processes related to dimers. However, quite similar attention has been given to problems where k-mers are randomly deposited on a surface. These studies are motivated by the important experimental background (see [9] and references therein). Furthermore, the numerical results of RSA of linear segments or "needles" deserve special attention. There are several contributions in the literature studying (a) their tendency to the jamming state [10–14], (b) their percolative behavior [15–17], and (c) the interplay between the jamming and percolative states [18–20]. In addition, it has been realized that continuum processes are obtained from lattice RSA processes in the limit of "large molecules" [9].

We consider a periodic square lattice of linear size L on which linear site and bond k-mers are independently deposited at random. The procedure is as follows. (1) A set of k linear nearest neighbor sites is randomly selected; if it is vacant, the site k-mer is then adsorbed on those sites. Otherwise, the attempt is rejected, and (2) a set of k nearest neighbor bonds (aligned along one of the lattice axes) is randomly chosen; if it is vacant, the bond k-mer is then dropped onto the lattice. Otherwise, the attempt is rejected. In any case, the procedure is iterated until N_s site k-mers and N_b bond k-mers are adsorbed and the desired concentrations ($p_s=kN_s/L^2, p_b=kN_b/2L^2$) are reached.

We may then define *site-and-bond* ($S \cap B$) and *site-or-bond* ($S \cup B$) percolation: in $S \cap B$, a cluster is considered to be a set of occupied bonds and sites in which the bonds are joined by occupied sites, and the sites are joined by occupied bonds. In $S \cup B$, a bond or site contributes to cluster connectivity independently of the occupation of its end points.

A typical phase diagram of site-bond percolation in the presence of multisite occupancy (dimers) is shown in Fig. 1. The critical curves corresponding to the $S \cap B$ and $S \cup B$ problems limit the percolating and nonpercolating regions, respectively. The main differences between the phase diagram in Fig. 1 and the corresponding one for classical site-bond percolation [4–6] are associated with the parameters p_s^j, p_b^j, p_s^c, and p_b^c, which will be presented in detail in Sec. II, along with the simulation scheme and the finite-size scaling theory. The phase diagram in the p_s-p_b space for linear site and bond k-mers on a square lattice is reported in Sec. III. Finally, our general conclusions are given in Sec. IV.

II. BASIC DEFINITIONS, SIMULATION SCHEME, AND FINITE-SIZE SCALING ANALYSIS

In the filling process, objects of finite size (k-mers) are randomly deposited (irreversibly adsorbed) on an initially empty substrate or lattice with the restriction that they must not overlap with previously added objects. Due to the blocking of the lattice by the already randomly adsorbed elements, the limiting or jamming coverage $p_s^j=p_s(t=\infty)$ [$p_b^j=p_b(t=\infty)$] is less than that corresponding to the close packing [p_s^j (p_b^j)<1]. Note that $p_s(t)$ [$p_b(t)$] represents the fraction of total site (bond) lattice covered at time t by the deposited

*Electronic address: mdolz@cabbat1.cnea.gov.ar
†Electronic address: fnieto@unsl.edu.ar
‡Author to whom correspondence should be addressed. Electronic address: antorami@unsl.edu.ar

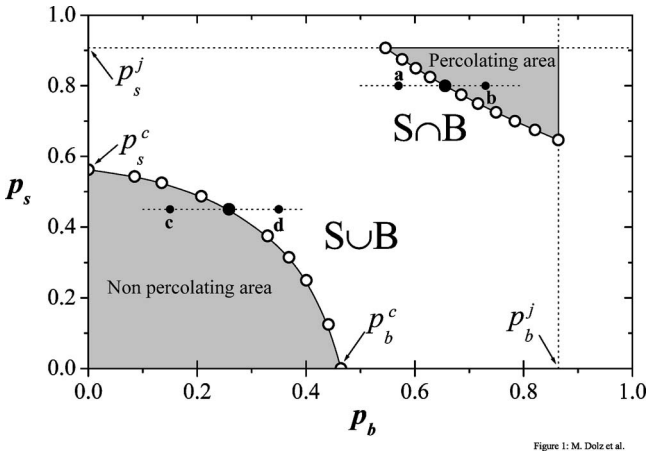

FIG. 1. Phase diagram (in the p_s-p_b parameter space) corresponding to the dimer site-bond percolation problem on square lattices.

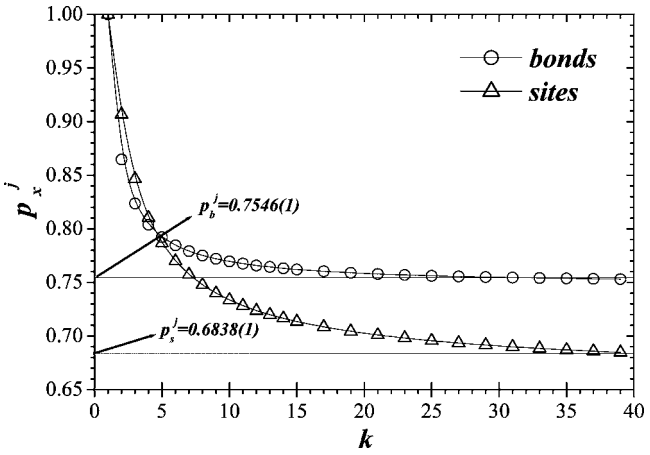

FIG. 2. Jamming coverage as a function of k for linear site k-mers (open circles) and linear bond k-mers (filled circles) on square lattices. The asymptotic limits $p_s^j(\infty)=0.6838(1)$ and $p_b^j(\infty)=0.7546(1)$ are shown.

objects. Consequently, $p_s(p_b)$ ranges from 0 to $p_s^j(p_b^j)$ for objects occupying more than one site and the total area in the p_s-p_b phase diagram is $p_s^j p_b^j$ (see Fig. 1). An extensive overview of this field can be found in the excellent work by Evans [9] and references therein. More recently, leading contributions have been presented in Refs. [18–25] treating the relationship between the jamming coverage and the percolation threshold.

In order to predict the behavior of the system in the thermodynamic limit it is required that our long scale numerical simulations become independent of the k-mer size. A study of the finite-size effects allows us to make a reliable extrapolation to the $k\to\infty$ limit when the limit $L\to\infty$ is taken before. This tendency toward the thermodynamic limit ensures that both the kinetic and the jammed saturation state are nontrivial, which is an appropriate model for many physical, chemical, and biological processes where the microscopic steps are effectively irreversible (e.g., chemical bond formation) and where equilibration is not possible on the time scale of the experiment [9].

Another mathematically possible limits could also be analyzed. In fact, one could consider $L/k\to\text{const}$ [or $L/k\sim O(1)$]. In this framework, the values of the percolation threshold and the jamming coverage strongly depend on the selected constant. In the trivial case $L/k\to 1$, the jammed state corresponds to $p_s^j(k)=p_b^j(k)=1$ and the total area in the p_s-p_b phase diagram is $p_s^j p_b^j=1$ regardless of the value of k. A recent work, Ref. [26], claims "to be the first attempt to study percolation of polymers on a lattice with multiple bond occupancies in this particular scaling limit $[L/kO(1)]$" inspired in a particular experimental setup. On the other hand, percolation of linear k-mers on a lattice of constant size L has been treated. In this case, an abrupt increment of $p_c(k)$, which depends on L, is observed upon increasing k [27,28]. One fundamental feature is preserved in all these limits. This is that the quantities of interest are dependent on the lattice size L. On the contrary, our study is performed in the direction of Ref. [9], where the size of the linear k-mer can always be neglected as compared with the lattice size.

In order to calculate the jamming limits for different values of k, we use a standard Monte Carlo procedure [29]. At each Monte Carlo attempt, a k-uple of linear neighboring sites (bonds) is chosen at random. Then, the sites (bonds) are occupied provided that all of them are empty; otherwise the attempt is rejected. As in Ref. [29], the dimensionless Monte Carlo time variable t may therefore be defined by having one attempt per each element (sites and bonds) of the lattice in the unit time step $t=1$. Thus, for the N-element lattice, the time step $t=1$ corresponds to N deposition-attempt Monte Carlo steps described earlier. In the calculations, we use square lattices of 10^4k^2 sites ($2\times 10^4k^2$ bonds) and t runs up to no sites (bonds) for deposition are available. In addition, each data set was averaged over 5000 runs.

In Fig. 2, the jamming limits for linear site k-mers, $p_s^j(k)$, and linear bond k-mers, $p_b^j(k)$, are plotted as a function of k. At the beginning, for small values of k, the curves rapidly decrease. However, they flatten out for larger values of k and finally asymptotically converge toward a definite value as $k\to\infty$.

The behavior of the curves in Fig. 2 can be associated with a decreasing function. For each case, a saturation value can be found in the limit for $k\to\infty$. Thus, $p_s^j(\infty)=0.6838(1)$ and $p_b^j(\infty)=0.7546(1)$ for site and bond k-mers, respectively. As it will be shown below, the values of $p_s^j(k)$ and $p_b^j(k)$ allow us to calculate the extremes of the critical curves corresponding to the $S\cap B$ model. On the other hand, the critical curves corresponding to $S\cup B$ model varies between the point $[p_s^c(k),p_b=0.0]$ at the left and the point $[p_s=0.0,p_b^c(k)]$ at the right, where $p_s^c(k)[p_b^c(k)]$ represents the threshold percolation for pure site (bond) k-mers on square lattices.

In Fig. 3, the percolation thresholds for linear site k-mers and linear bond k-mers are plotted as a function of k. Each point was calculated by using Monte Carlo simulation and finite-size scaling theory according to the Yonezawa technique [17,30,31]. The results can be well correlated by mean of an exponentially decreasing function:

$$p_x^c(k)=p_x^c(\infty)+\Delta_x\exp(-k/\zeta_x)\quad\text{and}\quad\{x\equiv s,b\},\qquad(1)$$

$p_x^c(\infty)$, Δ_x, and ζ_x being fitting parameters. The fitting parameters obtained are the following: $p_s^c(\infty)=0.461(1)$, Δ_s

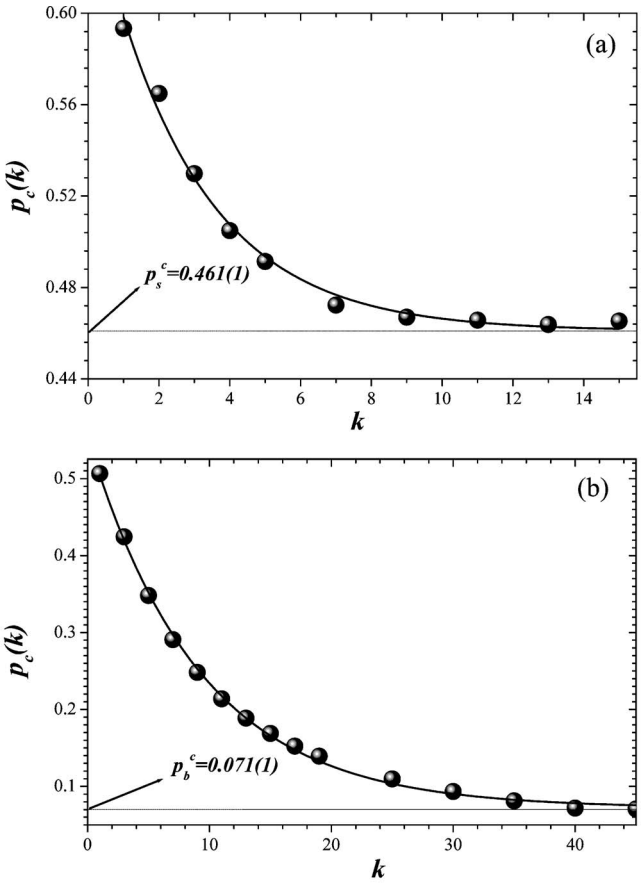

FIG. 3. Percolation threshold as a function of k for (a) linear site k-mers and (b) linear bond k-mers on square lattices. The behavior of the fitting curves are described according to Eq. (1). The asymptotic limits (a) $p_s^c(\infty)=0.461(1)$ and (b) $p_b^c(\infty)=0.071(1)$ are shown. The size of the points is larger than the corresponding error bars.

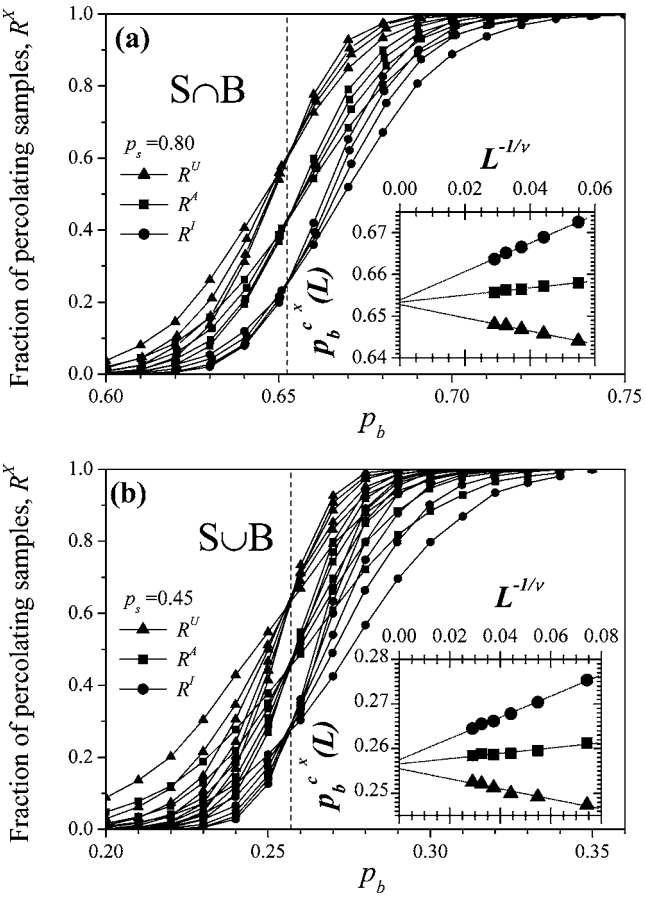

FIG. 4. (a) Fraction of percolating lattices for $S\cap B$ percolation of dimers, $p_s=0.80$, and variable p_b. Different criteria, U (triangles), I (circles), and A (squares), are used for establishing the spanning cluster. Vertical dashed lines denote the percolation threshold in the thermodynamic limit $L\to\infty$. In the inset, we present the extrapolation of p_b^c toward the thermodynamic limit according to the theoretical prediction given by Eq. (2). Circles, squares, and triangles denote the values of $p_b^c(L)$ obtained by using the criteria I, A, and U, respectively. The size of the points is lower than the corresponding error bars. (b) As part (a) for $S\cup B$ percolation of dimers, $p_s=0.45$, and variable p_b.

$=0.20(1)$, and $\zeta_s=2.8(2)$ for site k-mers, Fig. 3(a), and $p_b^c(\infty)=0.071(1)$, $\Delta_b=0.482(2)$, and $\zeta_b=9.2(2)$ for bond k-mers, Fig. 3(b).

Once the limiting parameters (p_s^j, p_b^j, p_s^c, and p_b^c) are calculated, each point corresponding to the critical curves $S\cap B$ and $S\cup B$ can be obtained by following the next steps: (a) the construction of the lattice for the desired fractions p_s and p_b of site k-mers and bond k-mers, respectively; (b) the mapping $\mathbf{L}\to\mathbf{L}'$ from the original site-bond lattice $\mathbf{L}$ to an effective bond lattice $\mathbf{L}'$ where each bond and its end point sites of $\mathbf{L}$ transform into a bond one of $\mathbf{L}'$ (the rules for the mapping have been detailed in Ref. [8]); and (c) the cluster analysis by using the Hoshen and Kopelman algorithm [32] on the effective bond lattice (the percolation threshold in the original and effective lattices must be equal). In the last step, the existence of a percolating island is verified. n runs of three such steps are carried out to obtain the probability $R=R_L^X(p_s,p_b)$ that a lattice composed of $L\times L(2L\times L)$ sites (bonds) percolates at concentration (p_s,p_b) [33]. Here, as in Ref. [30,31], the following definitions can be given according to the meaning of X: (a) $R_L^I(p_s,p_b)$ is the probability of finding a cluster that percolates both in a rightward *and* in a downward direction; (b) $R_L^U(p_s,p_b)$ is the probability of finding either a rightward *or* a downward percolating cluster; and (c) $R_L^A(p_s,p_b)\equiv\frac{1}{2}[R_L^R(p_s,p_b)+R_L^D(p_s,p_b)]\equiv\frac{1}{2}[R_L^I(p_s,p_b)+R_L^U(p_s,p_b)]$. Then the procedure is repeated for different values of (p_s,p_b), L, and k. A set of $n=5\times10^4$ independent samples is numerically prepared for each pair (p_s,p_b) and L/k ($L/k=8,16,24,32,40,48,56$).

In Fig. 4(a), the probabilities R_L^I (circles), R_L^U (triangles), and R_L^A (squares) are presented for dimer $S\cap B$ percolation, a fixed value of p_s (=0.80), and variable p_b. As can be observed, curves corresponding to different sizes cross each other at a unique universal point, which depends on the criterion X used, and those points are located at very well defined values on the p_b axes determining the critical percolation threshold p_b^c for each p_s (in this case $p_s=0.80$).

The finite-size scaling theory allows for another efficient route to estimate p_b^c from the extrapolation of the positions $p_b^{cX}(L)$ of the maxima of the slopes of R_L^X. For each criterion one expects that [33]

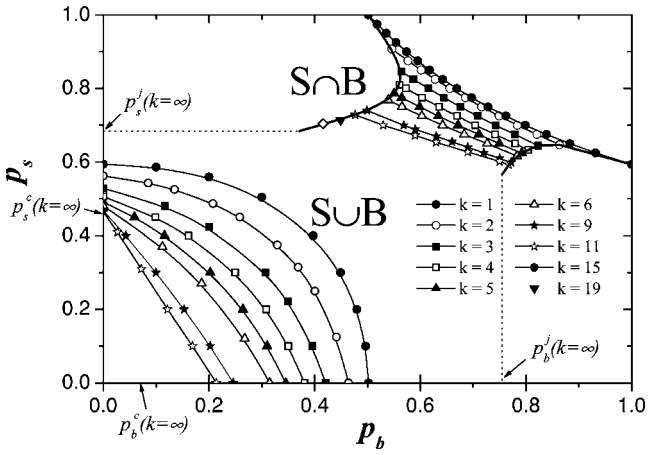

FIG. 5. Phase diagrams (in the p_s-p_b parameter space) corresponding to the k-mer site-bond percolation problem on square lattices for different values of k as indicated. The size of the points is larger than the corresponding error bars.

$$p_b^{cX}(L) = p_b^c + A^X L^{-1/\nu} \tag{2}$$

where A^X is a nonuniversal constant and ν is the critical exponent of the correlation length. The inset in Fig. 4(a) shows the extrapolation toward the thermodynamic limit of $p_b^{cX}(L)$ according to Eq. (2) for different criteria. This is done with $\nu=4/3$, since our model belongs to the same universality class as random percolation [8,17], as expected. Several conclusions can be obtained from the figure: (a) all the curves are well correlated by a linear function, (b) they have a quite similar value for the ordinate in the limit $L\to\infty$, and (c) the fitting determines a different value of the constant A depending on the type of criterion used. It is also important to note that $p_b^{cA}(L)$ gives an almost perfect horizontal line which is a great advantage of the method because it does not require precise values of critical exponent ν in the process of estimating percolation thresholds. The maximum of the differences between $|p_b^{cI}(\infty)-p_b^{cA}(\infty)|$ and $|p_b^{cU}(\infty)-p_b^{cA}(\infty)|$ gives the error bar for each determination of p_b^c.

The procedure done in Fig. 4(a) is repeated for the dimer $S\cup B$ percolation, a fixed value of p_s (=0.45), and variable p_b. The results are shown in Fig. 4(b).

It is worth noticing that the analysis in Fig. 4(a) [4(b)] corresponds to sequences of Monte Carlo simulations through the $(a-b)[(c-d)]$ path in Fig. 1. In general, from the point of view of calculations, we move along $(a-b)$-like horizontal paths. In other words, we set p_s=constant and vary p_b [34].

III. PHASE DIAGRAM

The finite-size scaling analysis (discussed in Sec. II) has been used in the whole range of the variables p_s and p_b in order to determine the percolation thresholds and the phase diagrams for different sizes of the percolating species ranging between $k=2$ and 11. Thus, the resulting p_s-p_b phase diagrams for k-mer site-bond percolation are shown in Fig. 5, in comparison with the standard site-bond percolation for monomers.

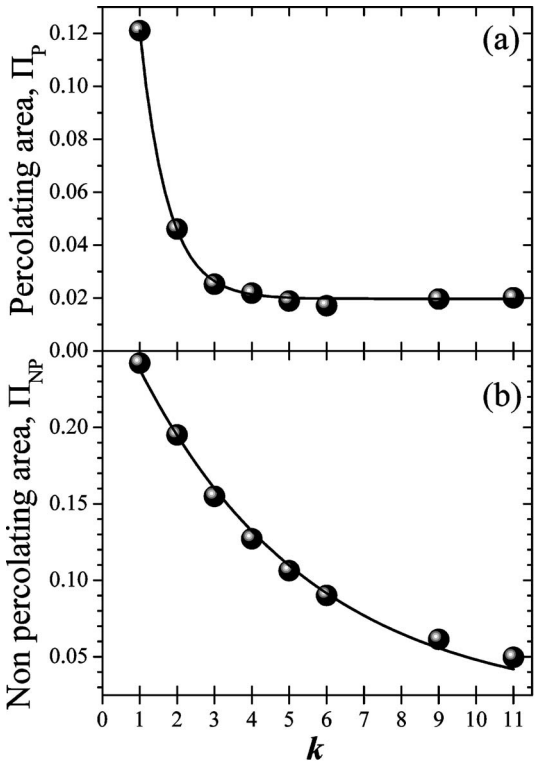

FIG. 6. (a) [(b)] Percolating (nonpercolating) area as a function of k for the k-mer site-bond percolation problem on square lattices. The behavior of the fitting curve is described according to Eq. (3). The asymptotic limit is shown.

The critical curves corresponding to the $S\cap B$ model are limited by $p_s^j(k)$ and $p_b^j(k)$, upper and lower extremes, respectively. The two envelope curves formed by those points are shown as solid thick lines in Fig. 5. On the other hand, the coexistence curves corresponding to the $S\cup B$ model vary between the points $[p_s^c(k), p_b=0.0]$ at the left and the points $[p_s=0.0, p_b^c(k)]$ at the right. These features represent one of the most important differences between the percolation problem in the presence of single and of multisite occupancy. For both cases considered here ($S\cap B$ and $S\cup B$) and k ranging between 1 and 11, the critical curve tends to be a straight line upon increasing the k-mer size. This effect is more pronounced for the $S\cap B$ case, where a linear coexistence curve is reached just for $k>5$, while values of $k>9$ are needed to show a similar feature in the case of $S\cup B$.

The extremes of the phase boundary can be calculated in the limit $k\to\infty$ as follows. For the $S\cap B$ case, the left (right) extreme point is obtained from the crossing between the horizontal (vertical) line $p_s^j(\infty)[p_b^j(\infty)]$ and the corresponding envelope curve described above. In the case of $S\cup B$, the extremes are obtained straightforwardly $\{[p_s^c(k=\infty), p_b=0.0]$ at the left and $[p_s=0.0, p_b^c(k=\infty)]$ at the right$\}$. However, the complete determination of the line for the coexistence curve should require either an extensive numerical simulation with systems of larger sizes (beyond our present computational facilities) or an analytical argument supporting the prediction that the coexistence curve tends to be linear for $k\to\infty$ as was shown for $9<k<11$ (out of our present

reach). It is important to emphasize that the behavior of the percolation threshold as a function of the parameters of the system is still now an open problem and only empirical relations exists there [35].

As can be observed, the areas of the percolating and nonpercolating regions diminish with respect to the corresponding ones for standard site-bond percolation. Thus, the percolating region Π_P and the nonpercolating area Π_{NP} are exponentially decreasing functions of k [see Figs. 6(a) and 6(b), respectively]. In fact, the points of the figures are well correlated with the following expression (dashed line in the figures):

$$\Pi_x(k) = \Pi_x(\infty) + A_x \exp(-k/\kappa_x) \quad \text{and} \quad \{x \equiv s,b\}. \quad (3)$$

According to Eq. (3) the fitting parameters for Fig. 6(a) are $\Pi_P(\infty)=0.0198(4)$, $A_P=0.397(3)$, $\kappa_P=0.73(2)$. Results for the nonpercolating area, Fig. 6(b), show a slower convergence than the case discussed before, the parameters being $\Pi_{NP}(\infty)=0.0164(2)$, $A_{NP}=0.275(4)$, and $\kappa_{NP}=4.63(7)$.

IV. CONCLUSIONS

In this work, the phase diagram of the site-bond percolation problem with multisite occupancy is addressed. The phase transition involved in the problem has been studied by using finite-size scaling theory.

The main characteristics of the phase diagrams obtained are the following. (1) The jamming coverage plays an important role in the system considered here. In fact, the critical curves corresponding to $S \cap B$ model are limited by the envelope functions $p_s^j(k)$ and $p_b^j(k)$. (2) The critical curves corresponding to $S \cup B$ model vary between the point $[p_s^c(k), p_b=0.0]$ at the left and the point $[p_s=0.0, p_b^c(k)]$ at the right. (3) In both analyzed cases, $S \cap B$ and $S \cup B$, the coexistence curves for values of k in the range $5<k<11$ tend to be straight lines. (4) The percolating and nonpercolating areas present exponentially decreasing behavior as a function of k, which allows one to predict their values for $k \to \infty$.

Finally, the present study encourages us to (a) develop an analytical approximation for understanding the shape of the coexistence curves and (b) determine the phase diagram of the site-bond percolation in different geometries and for nonlinear k-mers. This work is in progress.

ACKNOWLEDGMENTS

This work was made possible by CONICET (Argentina) and the Universidad Nacional de San Luis (Argentina) under Project No. 322000.

[1] H. L. Frisch and J. M. Hammersley, J. Soc. Ind. Appl. Math. **11**, 894 (1963)
[2] P. Agrawal, S. Render, P. J. Reynolds, and H. E. Stanley, J. Phys. A **12**, 2073 (1979).
[3] H. Nakanishi and J. Reynolds, Phys. Lett. **71A**, 252 (1979).
[4] M. Yanuka and R. Englman, J. Phys. A **23**, L339 (1990).
[5] C. Tsallis and A. C.N. de Magalhães, Phys. Rep. **268**, 305 (1996).
[6] Y. Y. Tarasevich and S. C. van der Marck, Int. J. Mod. Phys. C **10**, 1193 (1999).
[7] A. Coniglio, H. E. Stanley, and W. Klein, Phys. Rev. Lett. **42**, 518 (1979).
[8] M. Dolz, F. Nieto, and A. J. Ramirez-Pastor, Eur. Phys. J. B **36**, 391 (2005).
[9] J. W. Evans, Rev. Mod. Phys. **65**, 1281 (1993).
[10] Jian-Sheng Wang and Ras B. Pandey, Phys. Rev. Lett. **77**, 1773 (1996).
[11] J. D. Sherwood, J. Phys. A **23**, 2827 (1990).
[12] R. D. Vigil and R. M. Ziff, J. Chem. Phys. **93**, 8270 (1990).
[13] R. M. Ziff and R. D. Vigil, J. Phys. A **23**, 5103 (1990).
[14] G. Tarjus and P. Viot, Phys. Rev. Lett. **67**, 1875 (1991).
[15] Y. Leroyer and E. Pommiers, Phys. Rev. B **50**, 2795 (1994).
[16] B. Bonnier, M. Honterbeyrie, Y. Leroyer, C. Meyers, and E. Pommiers, Phys. Rev. E **49**, 305 (1994).
[17] V. Cornette, A. J. Ramirez-Pastor, and F. Nieto, Eur. Phys. J. B **36**, 391 (2003).
[18] G. Kondrat and A. Pekalski, Phys. Rev. E **63**, 051108 (2001).
[19] G. Kondrat and A. Pekalski, Phys. Rev. E **64**, 056118 (2001).
[20] F. Rampf and E. V. Albano, Phys. Rev. E **66**, 061106 (2002).
[21] H. S. Choi, J. Talbot, G. Tarjus, and P. Viot, Phys. Rev. E **51**, 1353 (1995).
[22] N. Vandewalle, S. Galam, and M. Kramer, Eur. Phys. J. B **14**, 407 (2000).
[23] M. Porto and H. E. Roman, Phys. Rev. E **62**, 100 (2000).
[24] E. S. Loscar, R. A. Borzi, and E. V. Albano, Phys. Rev. E **68**, 041106 (2005).
[25] P. Danwanichakul and E. D. Glandt, J. Colloid Interface Sci. **283**, 41 (2005).
[26] M. Gopalakrishnan, B. Schmittmann, and R. K.P. Zia, J. Phys. A **37**, L337 (2004).
[27] Y. Leroyer and E. Pommiers, Phys. Rev. B **50**, 2795 (1994).
[28] B. Bonnier, M. Honterbeyrie, Y. Leroyer, C. Meyers, and E. Pommiers, Phys. Rev. E **49**, 305 (1994).
[29] V. Privman and P. Nielaba, Europhys. Lett. **18**, 673 (1992).
[30] F. Yonezawa, S. Sakamoto, and M. Hori, Phys. Rev. B **40**, 636 (1989).
[31] F. Yonezawa, S. Sakamoto, and M. Hori, Phys. Rev. B **40**, 650 (1989).
[32] J. Hoshen and R. Kopelman, Phys. Rev. B **14**, 3438 (1976); J. Hoshen, R. Kopelman, and E. M. Monberg, J. Stat. Phys. **19**, 219 (1978).
[33] D. Stauffer, *Introduction to Percolation Theory*, 2nd ed. (Taylor & Francis, London, 1994).
[34] The critical point corresponding to $p_b=p_b^j$ is obtained for fixed p_b and variable p_s.
[35] Y. Y. Tarasevich and S. C. van der Marck, Int. J. Mod. Phys. C **10**, 1193 (1999).